CellPress

Trends in Chemistry

Review

Shape-controlled synthesis of metal nanocrystals: mind the surface heterogeneity

Quynh N. Nguyen,[1] Ruhui Chen,[1] and Younan Xia[1,2,*]

Shape-controlled metal nanocrystals have attracted growing interest due to their enhanced catalytic performance, cost-efficiency, and well-defined features for mechanistic investigations. However, the ultimate potential of these nanocrystals is limited by their surface heterogeneity. This review delves into the intricacies of surface heterogeneity, examining its role in dictating the sites for atom deposition and thereby the growth pattern of metal nanocrystals during colloidal synthesis. We also highlight the critical role of surface diffusion in preserving or overriding the impacts of surface heterogeneity, alongside the dynamic nature of surface structure throughout nanocrystal growth. Understanding and controlling the surface heterogeneity of nanocrystals are essential to the development of advanced catalytic materials.

Highlights

Shape-controlled synthesis offers a powerful tool to engineer the properties of nanocrystals, enhancing their catalytic performance while bridging the gap between surface science and industrial catalysis.

Surface heterogeneity in nanocrystals, arising from defects, variations in coordination number, diversity of facets, and differences in densities of capping ligands, is vital in directing atom deposition, ultimately dictating the shape or morphology.

Site-selected growth, a precise control of atom deposition on specific sites, offers a versatile route to the synthesis of well-defined nanocrystals.

The interplay between atom deposition and surface diffusion, influenced by factors including the type of facet, the capping agent, and temperature, is crucial in determining the final shape of nanocrystals.

Investigation of the dynamic nature of surface inhomogeneity during nanocrystal growth, storage, and application is key to understanding the relationship between surface features and catalytic performance.

Quest for well-defined catalytic materials

Catalysis has been a vital driving force in the global economy for almost a century, underpinning over 85% of the chemical industry [1]. Specifically, more than 80% of these processes rely on heterogeneous catalysts comprising metal nanoparticles on solid supports [2]. Despite their commercial success, heterogeneous catalysts have long been plagued by **surface heterogeneity** (see Glossary). Metal nanoparticles are typically covered by atoms in various coordination environments, including those situated on corners, edges, and faces [3,4]. The presence of defects such as atomic steps, kinks, vacancies, stacking faults, and twin boundaries further complicates the explanation of such catalytic materials [5,6]. Contrary to homogeneous catalysts, it is challenging to interpret the complex surface structures to define the 'active site' of commercial heterogeneous catalysts, let alone the difficulty of elucidating the working mechanism on their atomistic level. Exacerbating the situation, essentially all industrial catalysts are prepared via impregnation, involving the deposition of a precursor on the support followed by pyrolysis and reduction at elevated temperatures and under differing environments [3]. The as-prepared nanoparticles are so poorly defined and broadly distributed that it is almost impossible to identify two particles of identical size, surface structure, and interaction with the support.

To address this heterogeneity issue, researchers have pivoted toward model catalysts based on single-crystal substrates or thin films with well-defined atomic structures on the surface [7]. Such endeavors have evolved into a prolific research area known as surface science [8]. Fundamental research in this field has elucidated the dependence of catalytic activity/selectivity on the surface arrangement of atoms [9–11]. However, single-crystal substrates naturally introduce a 'materials gap' between industrial catalysis and surface science. This gap can be potentially closed by switching to metal nanocrystals with well-controlled shapes [12,13]. With their sizes controlled at a scale comparable with the nanoparticles commonly found in industrial catalysts, metal nanocrystals can be synthesized with uniform and well-defined surface structures by controlling their shapes [14–18]. These advanced nanomaterials provide a new class of well-defined substrates for surface science while offering an opportunity to enhance the performance of catalytic

[1]School of Chemistry and Biochemistry, Georgia Institute of Technology, Atlanta, GA 30332, USA
[2]Wallace H. Coulter Department of Biomedical Engineering, Georgia Institute of Technology and Emory University, Atlanta, GA 30332, USA

*Correspondence:
younan.xia@bme.gatech.edu (Y. Xia).

systems. Notable examples include the remarkable enhancement in activity and selectivity of Au rhombohedra enclosed by {110} facets relative to octahedral counterparts covered by {111} facets toward the electrochemical reduction of CO_2 to CO [19]. This improved performance was attributed to the increased binding affinity of the *COOH intermediate to {110} facets with undercoordinated surface atoms. This and other examples manifest the promise of shape-controlled metal nanocrystals in augmenting their catalytic performance toward structure-sensitive reactions [14].

Surface heterogeneity of shape-controlled metal nanocrystals

As a ubiquitous character of both natural and manmade materials, surface heterogeneity refers to the coexistence of sites differing in structural and chemical properties on a material's surface. For crystalline materials, differences in the atomic coordination environment naturally create surface heterogeneity. Owing to the presence of different types of facets, defects, and densities of capping ligands, the surface of a metal nanocrystal is intrinsically heterogeneous [14,20]. This heterogeneity can be leveraged to direct the shape evolution by controlling the sites at which the atoms are deposited [21]. Thus, even the same type of seed can evolve into nanocrystals with distinct shapes or morphologies depending on the growth pattern [13,22]. Deciphering how atoms are added onto and then incorporated into the surface of a growing seed is essential in controlling the morphology of final products. As illustrated by multiple examples below, maneuvering the surface heterogeneity of a nanocrystal is key to directing its shape evolution.

Single-crystal substrates

As a model system, single-crystal substrates offer insights into the structural features and surface heterogeneity of shape-controlled nanocrystals [23]. The relationship between surface heterogeneity and particle size can be visualized using a three-layer atomic model of the (100) surface of a single-crystal substrate comprising an *fcc* metal (Figure 1A). In this model, three types of surface atoms – found at corners, edges, and faces – are characterized by different coordination numbers (CNs) and bonding geometries with adjacent atoms. Specifically, the CNs are 3, 4, and 8, respectively, for the atoms situated at corners, edges, and faces. The proportions of these atoms depend on the lateral dimensions of the substrate. As the substrate decreases in lateral dimensions, the proportions of undercoordinated atoms at corners and edges increase. Thus, the surface of a small single-crystal substrate is markedly heterogeneous, with atoms on the outer layer sharing different CNs. By contrast, when the lateral dimension is sufficiently large, the surface can be considered more or less homogeneous, with surface atoms constituting over 90% of the surface. Besides the proportions of different types of surface atoms, heterogeneity can arise from surface defects such as terraces, steps, or kinks. When translating the properties of a bulk substrate into nanomaterials, the issue of surface heterogeneity becomes more apparent and should be scrutinized.

Shape-controlled nanocrystals

Contrary to the extended flat surface on a bulk crystal, the surface of a metal nanocrystal is intrinsically heterogeneous due to high proportions of undercoordinated atoms, in addition to those on the faces [14,24]. Similar to the trend observed in a single-crystal substrate, the fractions of different types of atoms on the surface correlate with particle size [25]. Such correlations can be quantified by varying the size of a metal nanocrystal having a known crystal structure and a well-defined shape. Taking a perfect nanocube comprising an *fcc* metal as an example, its surface is populated by atoms located at corners, edges, and {100} faces (Figure 1B). In general, atoms located on the corners and edges have lower CNs than those on the faces. As shown in Figure 1B, the ratio of corner and edge atoms relative to face atoms is inversely proportional to the size of the nanocube. When the edge length drops below 5 nm, the issue of surface

Glossary

Asymmetrical growth: the process in which the growth rates along the symmetry-related axes differ from each other, resulting in one or more corners, edges, or faces of a nanocrystal growing at a faster or slower rate than the rest, typically leading to the formation of nanocrystals with broken symmetry (one or more symmetry elements removed from their precursors, including the unit cell and/or the seed from which the nanocrystal grows).

Heterogeneous nucleation: a process involving the continuous deposition of atoms onto the surface of a growing nanocrystal or preformed seed in the growth solution to sustain its growth into nanocrystals without requiring a supersaturated environment.

Homogeneous nucleation: the first step of any synthesis without the introduction of preformed seeds that involves the aggregation or assembly of metal atoms into small clusters, commonly known as nuclei, once a supersaturated concentration of atoms in the solution phase is reached.

Oxidative etching: a redox reaction between the atoms on the surface of a nanocrystal and an etchant comprising an oxidant for the metal (e.g., O_2 from air) and a coordination ligand for the corresponding metal ions (e.g., halide ions released from the salt precursor or other additives). During etching, atoms are oxidized back to ions, which then coordinate with the ligand and are thus removed from the original structure.

Solution reduction: the metal ions in the precursor are directly reduced to atoms in the solution phase through collision and electron transfer with the reductant molecule, which then aggregate to generate nuclei through homogeneous nucleation or deposit onto the surface of the growing or preformed seeds through heterogeneous nucleation.

Surface heterogeneity: variation in physical and chemical properties across the surface of a material (e.g., atoms with different CNs situated at distinct faces, corners, edges, defects, and regions of nanocrystals with varying densities of surface ligands).

Surface ligands: ionic species, small molecules, or macromolecules adsorbed on a specific type of facet of growing nanocrystals, often referred to as a capping agent, to alter the surface energy landscape and impede or even

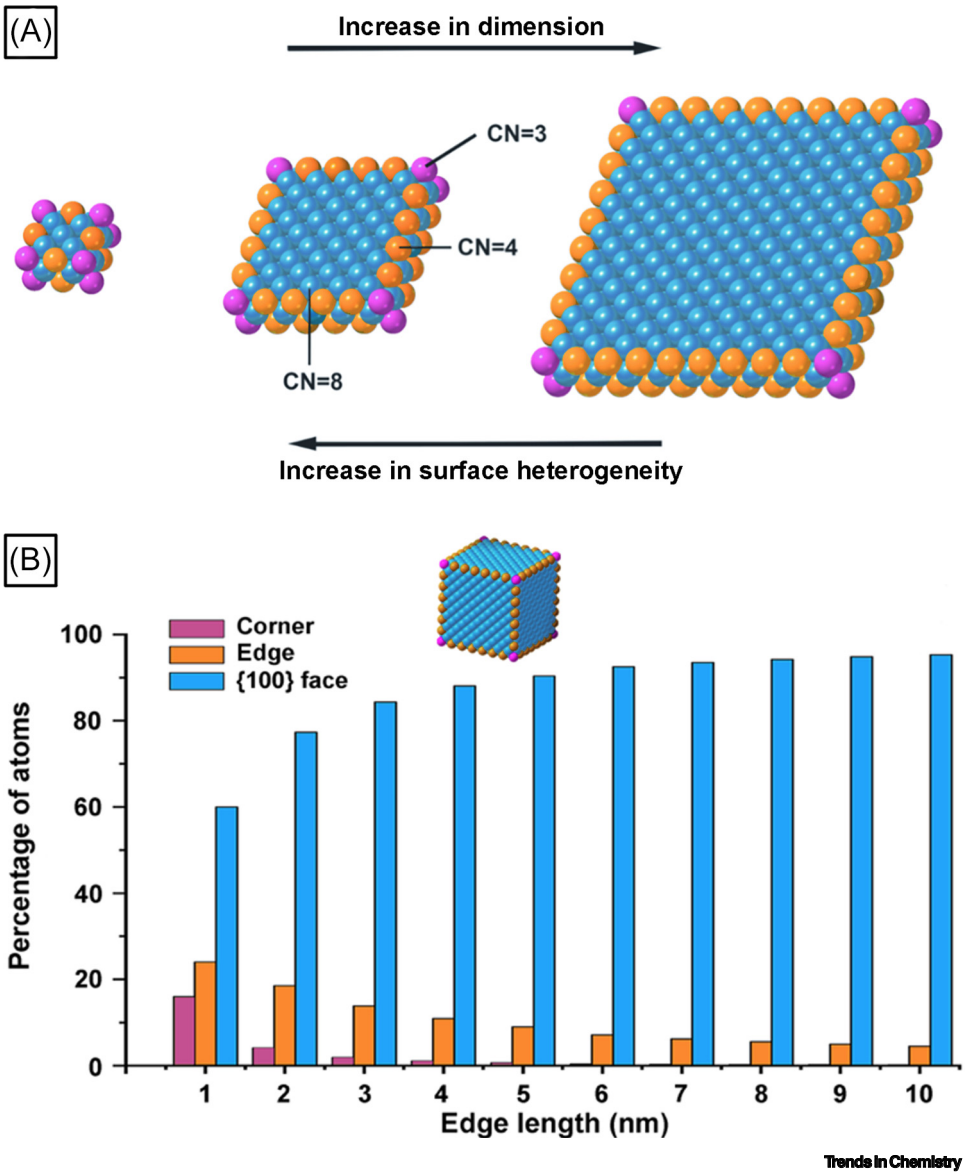

Figure 1. Effect of size on surface heterogeneity of a model substrate and a metal nanocrystal. (A) An atomic model showing the (100) surface of a single-crystal substrate comprising an *fcc* metal. The pink, orange, and blue colors denote atoms situated at corners, edges, and (100) faces, respectively. As the substrate increases in lateral dimensions, the proportion of undercoordinated atoms situated at corners and edges decreases while surface heterogeneity becomes less significant. (B) Percentage of surface atoms at corners, edges, and {100} faces of a perfect Pd nanocube as a function of edge length, indicating the dependence of surface heterogeneity on particle size. Abbreviation: CN, coordination number.

heterogeneity becomes significant, with corner and edge atoms dominating the surface. In other words, only above a certain size can the nanocube be approximated as having a (100) surface only with no surface heterogeneity. This trend highlights the importance of synthesizing shape-controlled nanocrystals of around 5 nm in size to optimize catalytic performance by balancing the expression of surface structures and thus area-specific activity [26–28]. The fractions of corner, edge, and face atoms and thereby variation of CNs can directly affect catalytic activity and selectivity by tuning the bond strength of reaction intermediates with the metal surfaces [24]. For example,

prohibit the deposition of atoms onto the capped facet, leading to the dominant expression of this facet on the products. They can also act as colloidal stabilizers to prevent nanocrystal aggregation.

Surface reduction: the precursor adsorbs onto the surface of an existing or preformed seed, followed by its chemical reduction to atoms through an autocatalytic process with a lower activation energy barrier due to the presence of locally existing surfaces acting as a 'catalyst' for the reduction process.

Symmetrical growth: the process in which all symmetry-related axes and thus the corresponding corners, edges, or facets of a nanocrystal grow at the same rate, typically giving rise to symmetry-preserved products (having the same symmetry as the unit cell and/or the seed).

the corner and edge sites of Pt truncated octahedra would become dominant for particles below 5 nm, compromising the specific activity toward oxygen reduction due to the strong binding of the O-containing intermediates to the undercoordinated sites [29,30]. For CO_2 reduction, small Pt nanocrystals with large proportions of corner and edge atoms tend to promote the charge transfer efficiency and thus enhance the generation of H_2 and CO, whereas the increased face atoms with high CNs in large nanocrystals exhibit higher CH_4 selectivity [31]. Thus, size reduction might not be the sole prerequisite for an effective catalyst when the active sites have a lower density and the populated surface sites have less intrinsic reactivity [32,33].

Undoubtedly, a real surface is more complex than the model system since an ideal surface does not exist in reality. Besides the different types of surface atoms, surface heterogeneity can arise from defects, such as point defects and incomplete surface layers commonly observed in metal nanocrystals prepared using colloidal synthesis. Point defects emerge when there are missing atoms in the unitary crystal structure, whereas incomplete surface layers originate from an inadequate supply of atoms and/or differences in mobility among adatoms and thus the formation of islands, vacancy pits, and atomic steps [34]. These surface defects have all been observed on the {100} side faces of Pd nanobars (Figure 2A,B), where atomic addition was responsible for the growth [35]. Additionally, defects at the corners and edges of a metal nanocrystal are more abundant than at the center of a flat face, leading to site-specific activity at different regions in the same particle [36]. A gradient of surface defect density was also discovered across the same flat face, which was substantiated by the gradual change in catalytic activity from the center of a face toward its corners and edges [36–38]. Surface defects, whose spatial distribution is strongly affected by the growth pattern of nanocrystals, can play influential roles in determining surface reactivity and should be considered when designing catalysts [34,39].

The shape of a nanocrystal can also affect surface heterogeneity by impacting the atomic arrangements on the faces. A combination of different low- and high-index facets, such as {100}, {110}, {111}, and {730}, can be found on nanocrystals with certain shapes. For example, the faces of a cuboctahedron are terminated by eight {111} and six {100} facets (Figure 2C,D) [14,40]. The atoms located at these faces have CNs of 9 and 8, respectively, equivalent to those of (111) and (100) surfaces for single-crystal substrates. Such diversity in facet type provides a flexible template to access nanocrystals with diverse shapes through protocols allowing maximal expression of a specific type of facet. Easily found in nanocrystals with a concave or convex structure, high-index facets, denoted by a set of Miller indices {hkl} with at least one of the indices being greater than one, are also a factor contributing to surface heterogeneity due to the presence of steps, kinks, and edges [41,42]. Because of their higher total surface energy relative to platonic counterparts, nanocrystals with high-index facets are typically obtained through kinetically controlled growth by choosing precursors and reductants with appropriate reactivity, introducing additives, and/or varying the temperature [43,44]. Furthermore, the shape of a nanocrystal can affect the coordination environment of a surface atom and thus surface heterogeneity from other aspects, including its second-nearest neighbors and surface curvature [45]. For nanocrystals sharing the same facet but different shapes, surface heterogeneity can be attributed to the involvement of planar defects, such as twin boundaries in decahedral and icosahedral nanocrystals (Figure 2E,F) [46] or stacking faults in nanoplates (Figure 2G,H) [40,47]. These defects at the boundary between adjacent subunits cause an uneven distribution of strain and a lopsided landscape of the surface energy, which ultimately influence the catalytic activity [48].

Surface ligands in a growth solution can complicate the surface heterogeneity of a nanocrystal [49]. Besides serving as colloidal stabilizers, surface ligands can act as capping agents by selectively binding to and thus passivating a specific type of facet to maximize its expression on the

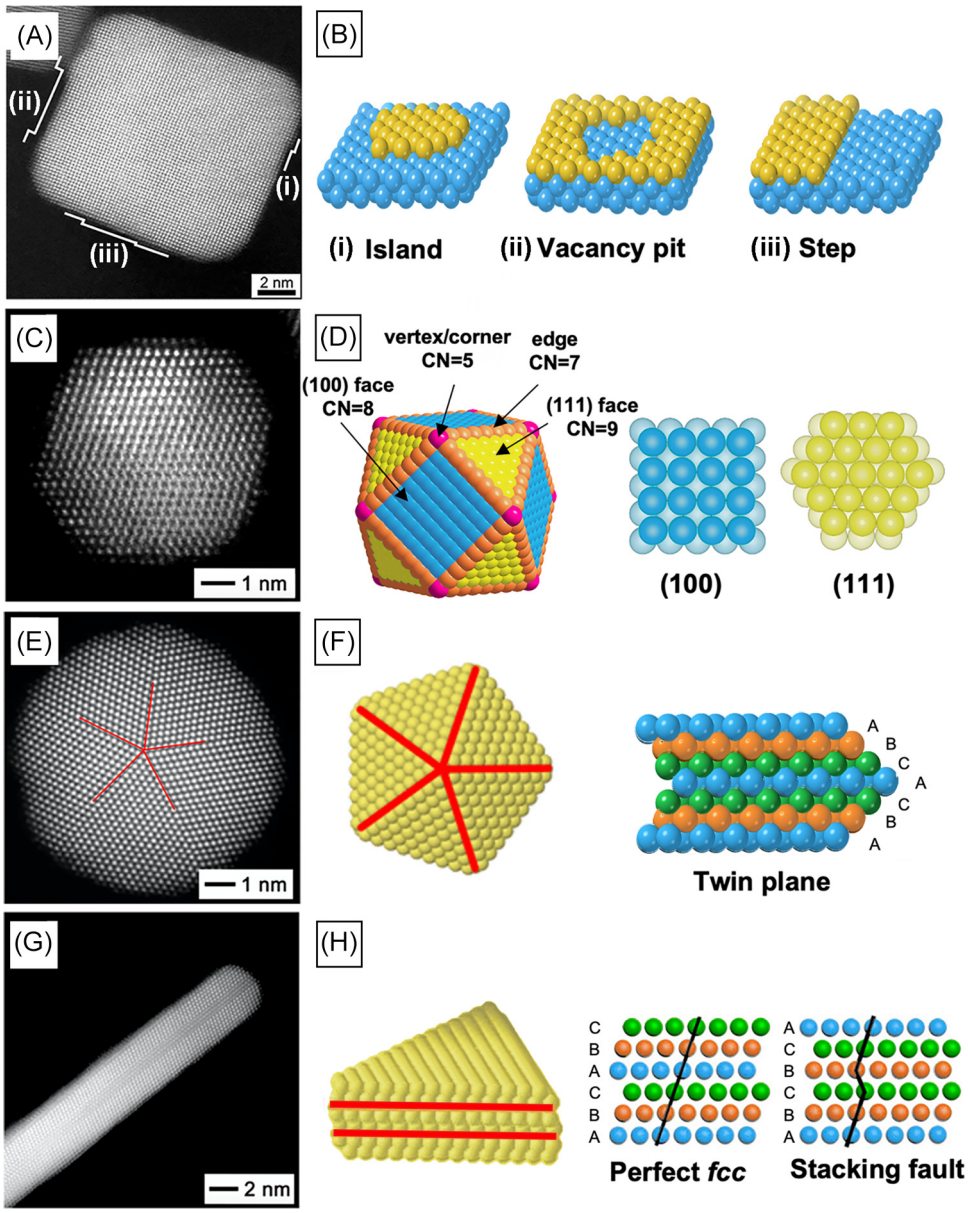

Figure 2. Surface heterogeneity of metal nanocrystals due to shapes, planar defects, and twin boundaries. (A,C,E,G) High-angle annular dark-field scanning transmission electron microscopy (HAADF-STEM) images of nanocrystals, with (B,D,F,H) the corresponding models and atomic arrangements on their faces covered by: (A,B) surface defects, (C,D) mix of different type of facets, (E,F) twin boundaries, and (G,H) stacking faults. The red lines indicate twin defects or stacking faults, while blue and yellow colors represent {100} and {111} facets, respectively. Adapted, with permission, from (A,B) [35], (C,G) [40], (D,F) [14], (E) [46], and (H) [47]. Abbreviation: CN, coordination number.

surface by reducing the surface energy. From a kinetic perspective, surface ligands can serve as a physical barrier to prevent the capped facet from receiving new atoms, influencing the outcome of colloidal syntheses. For example, poly(vinylpyrrolidone) can selectively adsorb onto Ag{100} facets whereas citrate tends to adsorb onto Ag{111} facets, leading to the formation of cubes and octahedra enclosed by these two types of facets, respectively [50,51]. Halides (e.g., Br^-

and I^- ions) are known for their selectivity in capping the {100} facets of most noble metals [49,52]. The introduction of different surface ligands and/or control of their coverage densities on various facets allow us to manipulate the corresponding surface energies and thus alter the surface heterogeneity of metal nanocrystals. Besides their versatile roles in shape-controlled synthesis, surface ligands can act as 'poisons' to limit the accessibility of active sites or 'facilitators' to improve the catalytic activity and/or selectivity [53].

Influence of surface heterogeneity on nanocrystal growth

Nanocrystal growth is a dynamic process involving the continuous deposition of atoms derived from the reduction of a precursor onto the surface of existing seeds, facilitating their evolution into nanocrystals with various shapes. In principle, the precursor can undergo reduction in the solution phase or on the particle surface, corresponding to **solution reduction** and **surface reduction**, respectively [54–56]. During the initial stage of a one-pot synthesis, solution reduction dominates due to the absence of preexisting surfaces. Thus, the precursor is reduced to atoms in the solution phase, which then aggregate into nuclei through **homogeneous nucleation**. Upon the formation of seeds, either *in situ* or introduced into the reaction solution, the newly generated atoms tend to grow from the existing surfaces through **heterogeneous nucleation**. Typically, surface reduction is more favorable during growth owing to its lower energy barrier and associated autocatalytic mechanism [21,57]. However, even during the growth stage, the continuous supply of precursor can cause the atom concentration to surpass the supersaturation threshold. In this case, additional homogeneous nucleation (or secondary nucleation) may be triggered, generating a new population of seeds and thus polydispersity of products. Lowering the reaction temperature and/or reducing the concentration or injection rate of the precursor to decelerate the kinetics can promote surface reduction over solution reduction, suppressing secondary nucleation and enhancing product uniformity [57–59]. While the two reduction pathways of a precursor are typically intertwined, they can be differentiated qualitatively based on the synthesis outcome or quantitatively by tracking the precursor concentration remaining in the solution over time [54,56]. Regardless of reduction pathway, continuous deposition of atoms onto a nanocrystal results in a highly dynamic surface energy landscape throughout growth.

If atomic addition prevails, the surface heterogeneity of seeds can affect the growth pattern of a nanocrystal at the atomic level. According to the collision model for thin film deposition, the atoms striking the surface may either bounce back or adhere to it [60]. Once deposited, the adatoms may desorb from the surface or undergo diffusion until they find the most stable site for incorporation. Experimental and theoretical studies have established that incoming atoms preferentially target sites with lower CNs (e.g., corners, edges) or higher surface energies (e.g., high-index facets, defects, sites under a high degree of strain, poorly capped regions) [61–66]. A quantitative analysis has also validated the influence of surface heterogeneity on the kinetics of surface reduction, leading to distinct growth rates for different sites on the seed surface and eventually the formation of nanocrystals with diverse shapes (Box 1) [57]. Such a deep understanding of site-selected growth arising from surface heterogeneity offers a viable route to nanocrystals with unique shapes or morphologies.

As the active center for various reactions, a high content of low-CN sites in a stable structure is desirable in catalyst design. From the thermodynamic perspective, it is challenging to produce and stabilize core-frame, frame, and concave nanocrystals featuring high-index facets lined with atomic steps due to the associated high surface energies [67,68]. Benefiting from surface heterogeneity, however, such nanostructures can be fabricated by confining atomic deposition to certain sites on a seed (e.g., corners, edges, defects) rather than a conformal shell on the entire surface. This strategy has been applied to produce core-frame or concave nanocrystals for

Box 1. Influence of surface heterogeneity on the kinetics of surface reduction and site-selected growth

Based on the Finke–Watzky model and Arrhenius plot, a quantitative study confirmed that the growth pattern and shape evolution of nanocrystals are related to surface heterogeneity, which influences the kinetics of surface reduction [57]. With capping-free Pd decahedral and icosahedral nanocrystals serving as seeds, concave structures with a tip protruding from each vertex were obtained upon the introduction of a Pd(II) precursor. Although all of the seeds are covered by {111} facets, the activation energy for surface reduction on the vertices of multiply twinned seeds (E_a = 25.8 and 21.1 kJ/mol for decahedral and icosahedral seeds, respectively) was significantly lower than that on the {111} facets of single-crystal octahedral seeds (E_a = 65.1 kJ/mol). This result quantitatively demonstrates that it is much easier for atom deposition to occur on the vertices of a multiply twinned seed instead of the {111} facets. This trend could be attributed to the low CNs of vertices and the surface strain associated with the slight expansion of each tetrahedral subunit to accommodate angular deficiency in decahedral and icosahedral construction [66]. Further study of surface reduction on capping-free single-crystal seeds with cubic and octahedral shapes suggested preferential growth of atoms on {100} facets with a half activation energy for surface reduction relative to that on {111} facets. The higher surface energy of {100} relative to {111} in the absence of capping agents made them a prior choice for the deposition of atoms [65]. Overall, the activation energy barrier to surface reduction was dependent on the surface structures, following the order {111} > {100} > vertex of a decahedron > vertex of an icosahedron. Such a quantitative understanding can be used to predict the growth pattern of other seeds with a more heterogeneous energy landscape and thus the shape taken by the final nanocrystals.

metals including Ag [69], Au [42], Pd [43,70], Pt [44,71], Rh [72], and some of their alloys [73,74]. For instance, Pd@Pt core-frame nanocubes were synthesized by capping the faces of Pd nanocubes with Br^- and thereby confining Pt deposition to corners and edges (Figure 3A,B) [71]. The success of this synthesis relies on simultaneous control over the limited supply of Pt atoms, preferential nucleation and growth of Pt from the corners and edges, and restricted surface diffusion to prevent the formation of a conformal shell. Because of their differing resistance to **oxidative etching**, Pd cores could be selectively removed to generate Pt nanoframes with a highly open structure (Figure 3C). The vertices of multiply twinned nanocrystals can also be selected as deposition sites due to their higher surface energies relative to edges and faces [75–77]. A recent study demonstrated site-selected deposition of Pt on the vertices of Pd icosahedral seeds for the generation of Pd–Pt great icosahedral nanocrystals (Figure 3D,E) [78]. The preferential deposition was ascribed to the slow reduction of the Pt(II) precursor through coordination with Br^- and the decelerated surface diffusion at room temperature, leading to the formation of multiply twinned Pt dots on the 12 vertices of each icosahedron.

Besides binding strength and preference, variations in the coverage density of surface ligands on certain regions can also be leveraged to promote site-selected growth. Taking nanoplate as an example, its corners had a higher degree of curvature than edges and faces, leading to a larger average distance between the ligands, easier access for atoms, and thus a lower energy barrier to growth at the corners (Figure 3F–H) [79]. The specific activation energy window for each site could be established by manipulating the difference in chemical potential (μ) of the growth solution and introducing distinct energy barriers (E) at different sites on the nanoplate (Figure 3I). Corner-selected ($E_c < \mu < E_e$) and edge-selected ($E_e < \mu < E_f$) growth was achieved using mPEG6 disulfide as a ligand with suitable length and binding affinity to establish different E values for growth selectivity while tuning the concentration of ascorbic acid as a reducing agent to control μ relative to E. As a common theme in all synthetic protocols, kinetically controlled mode is the deterministic switch to activate site-selected growth according to surface heterogeneity, preventing adatoms from rearranging to a lower-energy configuration (e.g., surface diffusion) to produce a conformal shell [65].

Role of surface diffusion in preserving or overriding surface heterogeneity

Surface diffusion of adatoms is a pivotal factor governing surface heterogeneity and consequently influencing the shape evolution of nanocrystals (Box 2) [80,81]. The final shape is ultimately determined by the relative rates of atom deposition ($V_{deposition}$) and surface diffusion ($V_{diffusion}$) [80,82]. An exemplary illustration is evident in the growth of a slightly truncated nanocube whose faces are

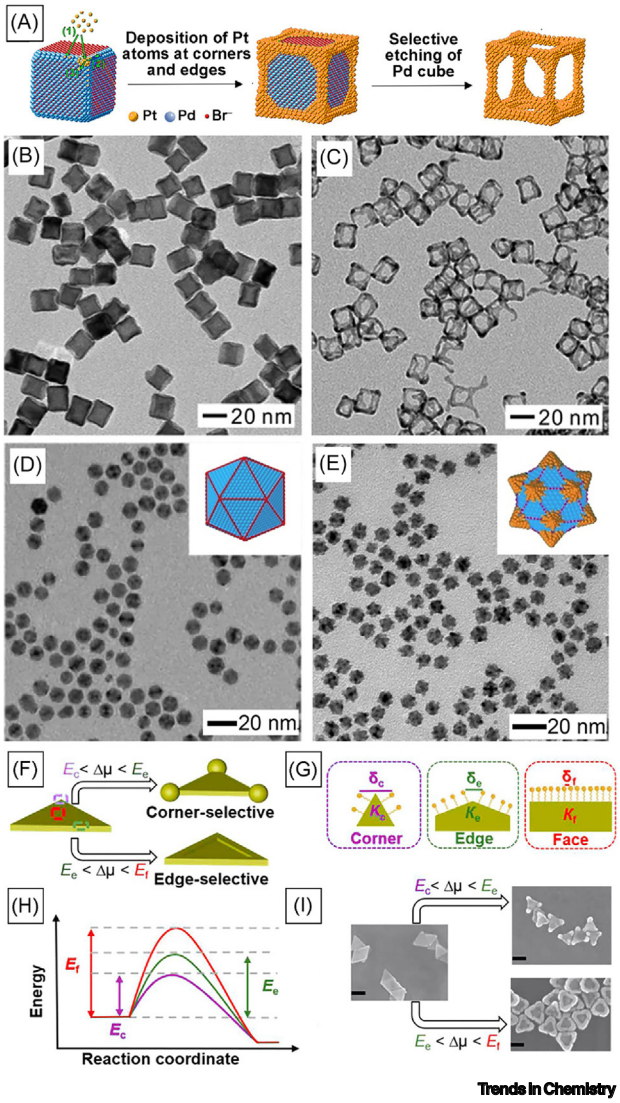

Figure 3. Effect of surface heterogeneity in directing site-selected growth on nanocrystals. (A) Schematic illustrating the preferential deposition of atoms at corners and edges of a cubic seed, resulting in a core-frame structure, followed by its transformation into a frame by removal of the core. (B,C) Transmission electron microscopy (TEM) images of the Pd@Pt core-frame cubes and Pt nanoframes. (D,E) TEM images of Pd icosahedra serving as seeds and Pd–Pt great icosahedral nanocrystals obtained through the preferential deposition of Pt on the vertices. The insets show atomic models of the corresponding particles, with red lines representing twin boundaries, while blue and orange colors denote Pd and Pt atoms, respectively. (F–I) Corner- and edge-selected overgrowth of Au nanocrystals. (F) The relationship between the supersaturation of the growth solution ($\Delta\mu$) and the energy barrier for nucleation (E) to achieve selected growth of Au on Au nanoplates. $\Delta\mu$ is defined as the driving force for nanocrystal growth, determined by the difference between chemical potential of the solute in solution (e.g., Au^0 atoms) and that of the solid crystal (e.g., Au seed). (G) Schematic illustrating different regions [corners (c), edges (e), and faces (f)] of a Au nanoplate with varying curvatures and thus different ligand densities. The higher the degree of curvature (K), the larger the average distance between the ligands (δ) (here, $K_c > K_e > K_f$, so that $\delta_c > \delta_e > \delta_f$). (H) General trend of the energy profile for nanocrystal growth in relation to the degree of curvature, where $E_c < E_e < E_f$. (I) Scanning electron microscopy (SEM) images showing corner- and edge-selected nucleation on Au nanoplates (bars, 100 nm). Adapted, with permission, from (A–C) [71], (D,E) [78], and (F–I) [79].

passivated by a capping agent for {100} facets (Figure 4A) [80]. The surface energies of various sites increase in the order of faces, corners, and edges owing to the differences in the CNs of the surface atoms and the presence of the capping agent. During synthesis, the atoms are deposited on the uncapped corners and edges. When $V_{deposition} > V_{diffusion}$, adatoms 'strike and stick' to the original sites due to the inadequate time for diffusion. This site-selected growth preserves and even enhanced surface heterogeneity, generating nanocubes with increasingly sharpened corners and edges, concave cubes, and even octopods depending on the extent of growth (Figure 4B i,ii). If $V_{deposition} < V_{diffusion}$, adatoms 'strike and slide' by diffusing from initially deposited corners and edges to faces. In this case, the surface heterogeneity of the original cube is overridden, generating a nanocrystal with a more homogeneous surface, including cubes of gradually enlarged size, cuboctahedra, and eventually octahedra enclosed by {111} facets (Figure 4B iii,iv).

Box 2. The role of surface diffusion in controlling the shape of metal nanocrystals

Surface diffusion is a thermally activated process that involves the motion of adsorbed atoms (adatoms) on a surface. Upon deposition at a specific site on the surface of a nanocrystal, the adatom can migrate to other regions through diffusion, altering the landscape of surface energy and thus the shape taken by the final product. The rate of surface diffusion (V_{diff}) can be expressed as $V_{diff} = D_0\, e^{-E_{diff}/RT}$, where D_0 is the pre-exponential factor, E_{diff} is the activation energy, R is the ideal gas constant, and T is the temperature [14]. According to this equation, the magnitude of V_{diff} is determined by E_{diff} and T. Specifically, E_{diff} represents the minimum energy required for an adatom to hop from one site to another, which is typically dependent on the local environment (e.g., the type of facet and the bonding energy between the surface atom and adatom) and the accessibility of the surface (e.g., the presence or absence of adsorbates). For example, theoretical calculations indicated that the value of E_{diff} for Rh adatoms to diffuse across a close-packed Rh(111) surface was 0.16 eV, but E_{diff} increased to 0.60 and 0.88 eV when diffusing on Rh(110) and (100) surfaces, respectively [81]. These values imply that the diffusion of Rh adatoms across Rh(111) would be much faster than either Rh(100) or Rh(110). In an experimental study, it was demonstrated that the selective capping of a Ag(100) surface by Cl^- could greatly slow the diffusion of Ag adatoms across the {100} facets of a truncated cubic nanocrystal, resulting in site-selected growth from the {111} and {110} facets for the formation of a nanocube with sharp corners and edges [52].

Once the surface heterogeneity of a seed is reinforced, the ratio between $V_{deposition}$ and $V_{diffusion}$ can serve as a simple metric to further manipulate its growth pattern (symmetrical vs asymmetrical) and thus the resultant shape. A fast $V_{deposition}$ that overwhelms $V_{diffusion}$ can lead to **asymmetrical growth** by introducing surface heterogeneity to a seed, generating nanocrystals with symmetry-

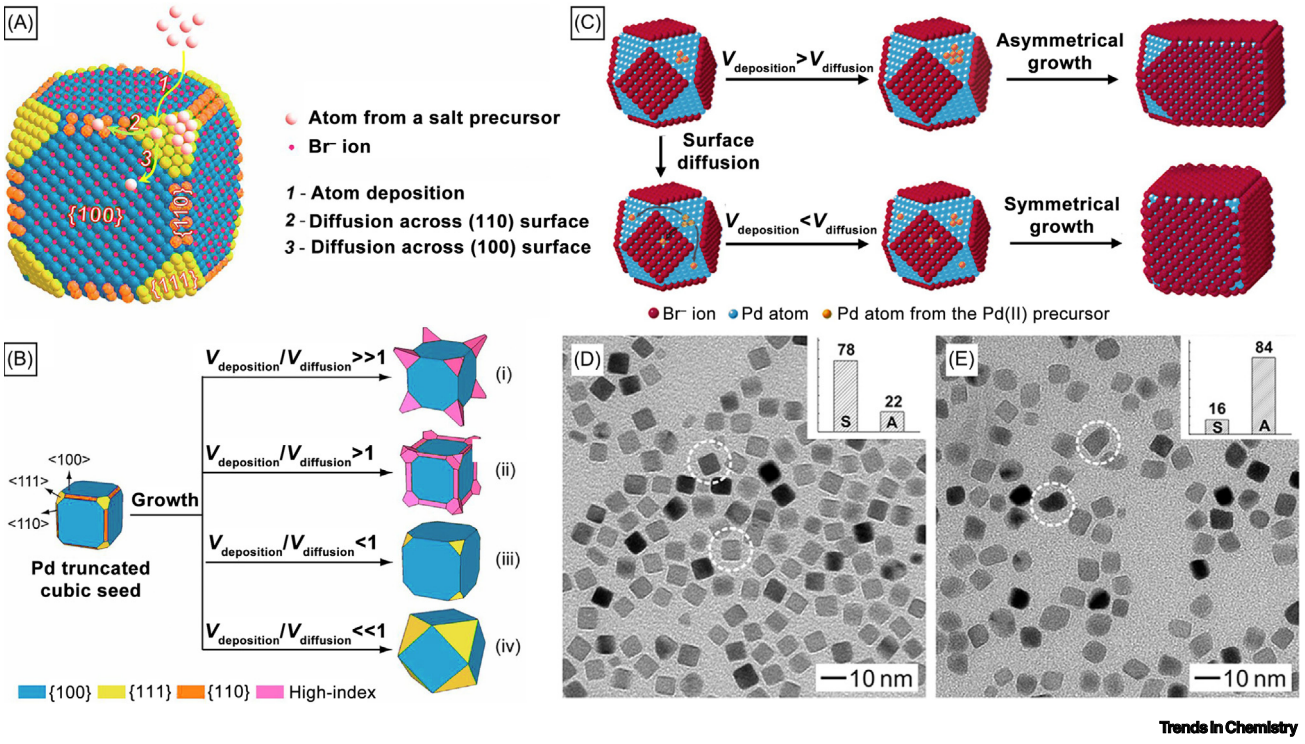

Figure 4. Influence of surface diffusion, relative to deposition, on the preservation or overriding of surface heterogeneity, and thus shape evolution and symmetry reduction. (A,B) Schematic illustrating (A) three possible sites for atom deposition and diffusion on the heterogeneous surface of a slightly truncated cubic seed in the presence of Br^- as a capping agent for {100} and (B) various growth pathways and the corresponding shapes expected for the growth of a cubic seed under different ratios of surface diffusion rate relative to deposition rate. (C) Schematic illustrating the effect of surface diffusion on the asymmetrical and symmetrical growth of a Pd cuboctahedral seed. (D,E) Transmission electron microscopy (TEM) images of Pd nanocrystals obtained by introducing Pd(II) of differing concentration at the same injection rate. The numbers of Pd(II) ions in each drop (normalized to the number of seeds in the growth solution) were (D) 4.7 and (E) 70.5, respectively, suggesting that a faster deposition rate relative to surface diffusion led to asymmetrical growth. The insets in (D,E) show the histogram distributions of the nanocrystals with symmetry-preserved (S) and symmetry-broken (A) shapes. Adapted, with permission, from (A,B) [80] and (C–E) [85].

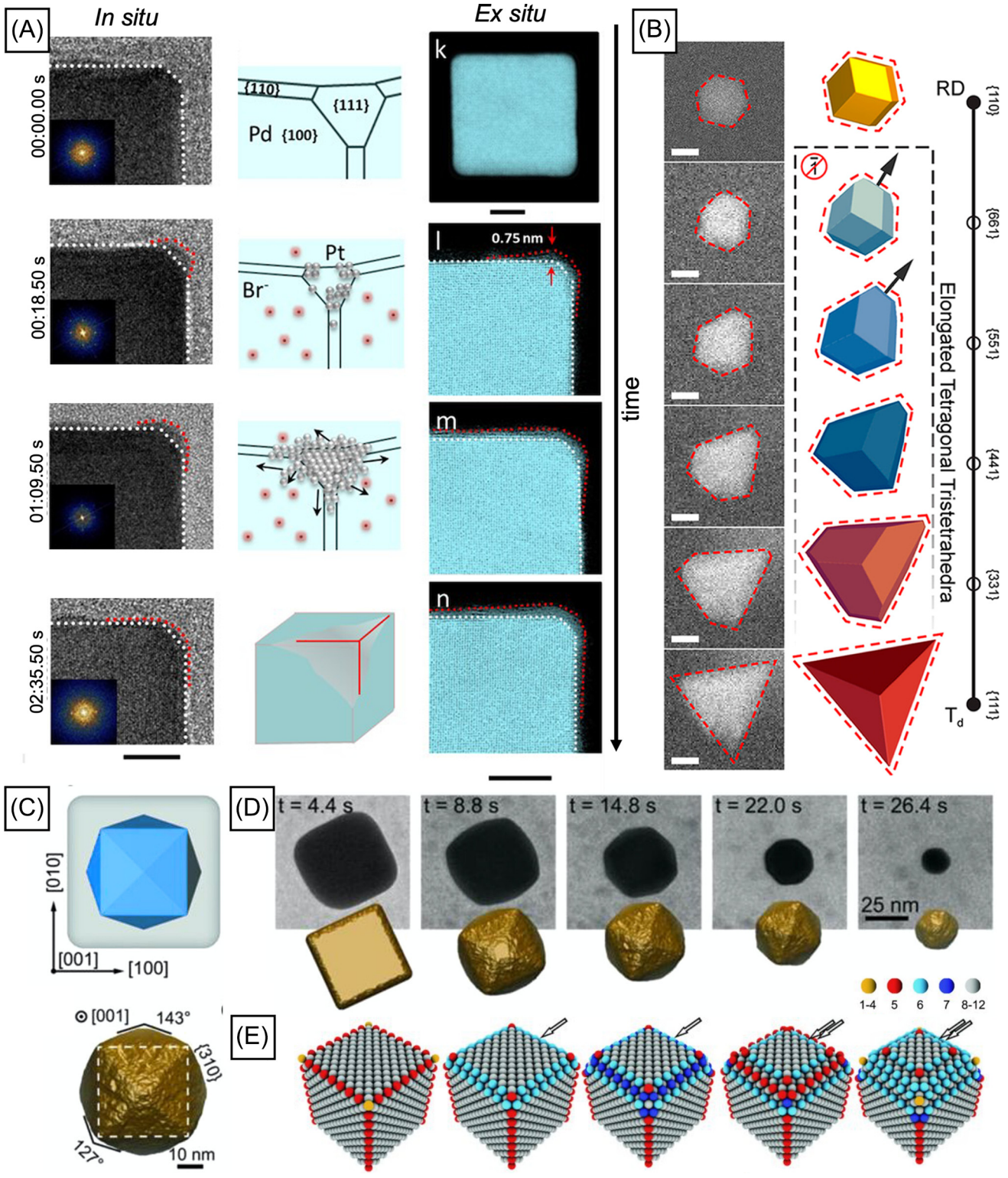

Trends in Chemistry

(See figure legend at the bottom of the next page.)

reduced shapes [22]. Since most noble metals crystallize in an *fcc* structure, their nanocrystals often follow a **symmetrical growth** pattern to adopt symmetry-preserved shapes such as cubes, octahedra, and cuboctahedra as confined by the cubic symmetry of the crystal lattice. Furthermore, the atoms on the same facets are equivalent in atomic arrangement and CN, making it difficult to achieve symmetry breaking in the growth process. In addition to the intrinsic high symmetry, the tendency of surface diffusion increases the difficulty of restricting adatoms to specific regions on a seed, hampering the asymmetrical growth. Therefore, precise control of $V_{deposition}$ relative to $V_{diffusion}$ is instrumental in generating products with reduced symmetry, which can be achieved by tuning the concentration of the precursor, its injection rate, and the temperature [83,84]. Using a syringe pump, dropwise addition of a precursor solution has emerged as the most robust and versatile method to keep the precursor concentration stable throughout a synthesis while maneuvering the deposition and diffusion rates responsible for switching between symmetrical and asymmetrical growth of Pd cuboctahedral seeds (Figure 4C) [85]. The supply of Pd atoms and thus $V_{deposition}$ could be controlled by varying the initial concentration of Pd(II) precursor in each injected droplet. Since the {100} facets of Pd cuboctahedra were passivated by Br^-, a limited number of Pd atoms generated from the first few droplets preferentially nucleated from some of the eight {111} facets on the seed. These activated facets served as active sites for subsequent growth due to their relatively high surface energy as they comprised undercoordinated atoms and were less passivated by capping agents. Even at a reduced supply of atoms due to a low concentration of precursor solution, adatoms would have enough time to migrate to adjacent {111} facets through surface diffusion once $V_{diffusion}$ became comparable with $V_{deposition}$. As a result, all eight {111} facets of cuboctahedral seeds were activated for symmetrical growth, producing symmetry-preserved nanocubes with larger sizes, accounting for 78% of the final particles (Figure 4D). By contrast, when increasing the Pd(II) concentration, the proportion of symmetry-broken products was increased, with 84% of them in the shape of elongated cubes (Figure 4E). Since a high Pd(II) concentration was used and a large number of atoms were generated as more droplets were introduced, there was inadequate time for all of the adatoms to diffuse to adjacent faces, and elongated nanocubes with atoms accumulated on some of the six faces were obtained. Similarly, elongated nanocubes could be generated by increasing the injection rate or decreasing the temperature to ensure that $V_{deposition}$ surpassed $V_{diffusion}$ [85]. Overall, symmetry breaking could be initiated and retained by maintaining a reduction rate slow enough to limit the number of deposition sites on the seed surface but fast enough to surpass surface diffusion. These strategies could be used to enable rational synthesis of nanocrystals with reduced symmetry, such as dimers, nanobars, nanorods, and nanowires [75,86]. Taking these findings together, the kinetics of surface diffusion are crucial in determining the landscape of surface heterogeneity for a growing nanocrystal and thereby its shape evolution. Both site-selected deposition and asymmetrical growth will vanish when surface diffusion outperforms deposition, shifting the shape evolution from kinetic to thermodynamic control.

Figure 5. Dynamic nature of surface structures as a result of atom deposition and diffusion, shape evolution, and size enlargement during nanocrystal growth and storage. (A) Time-elapsed *in situ* transmission electron microscopy (TEM) and *ex situ* high-angle annular dark-field scanning transmission electron microscopy (HAADF-STEM) images recorded during Pt deposition and diffusion on Pd cubic seeds whose faces were capped by Br^-. The corresponding models showing the heterogeneous nature of the surface during the formation of Pd@Pt core-shell nanocrystals. (B) In situ *TEM* images and the corresponding models showing facet development during the shape transformation and size enlargement from a rhombic dodecahedron to a tetrahedron. (C–E) Transition of a cube to a tetrahexahedron with a high-index {310} facet during kinetically controlled oxidative etching: (C) model of a cube (gray) and the intermediate tetrahexahedron shown internally (blue) and individually with labeled zone axis and calculated {hk0} facet angles; (D) time-lapse TEM images with corresponding snapshots from Monte Carlo simulations; and (E) atomic models showing the dissolution of a Au nanocube in a controlled redox environment inside a graphene liquid cell. Individual atoms in the atomic models are color-coded according to their coordination number, with color-coded legends shown on the bottom right. Adapted, with permission, from (A) [90], (B) [91], and (C–E) [95].

Dynamic nature of surface heterogeneity during nanocrystal growth

At the atomic level, the surface landscape of a growing nanocrystal is intrinsically dynamic, constantly adapting to the influx of newly deposited atoms and their migration, shape transformation, and size enlargement. The evolving surface structure during nanocrystal growth has been elucidated by tracking their growth trajectories using various characterization techniques [87–89]. Using *in situ* liquid-cell transmission electron microscopy (TEM), for example, atom deposition and diffusion dynamics were found to modulate the surface heterogeneity during the formation of Pd@Pt core-shell nanocubes (Figure 5A) [90]. When the faces of a cubic seed were capped by Br^-, Pt atoms preferentially nucleated from corners and then diffused to edges and faces to create a uniform shell once the deposited layer on the Pd{111} facet reached a threshold thickness. The facet development contributing to the dynamic nature of the nanocrystal surface was also revealed through a symmetry-breaking mechanism during the transition of a rhombic dodecahedron to a tetrahedron (Figure 5B) [91]. The surface underwent constant reconstruction through simultaneous growth of all {110} faces of a rhombic dodecahedron into a series of high-index ({661}, {551}, {441}, and {331}) and finally {111} facets, accompanied by the gradual elongation of tetragonal tristetrahedral intermediates through tip-selective growth. The interaction between surface ligands and the nanocrystal surface during synthesis further accentuates the intricacy of surface heterogeneity [49]. To this end, Fourier-transform IR spectroscopy, X-ray photoelectron spectroscopy, surface-enhanced Raman scattering, and energy-dispersive X-ray mapping have been extensively employed to identify the surface ligands [92,93], while their quantitative information has been obtained through UV-visible spectroscopy and inductively coupled plasma mass spectrometry [94].

Besides growth-related factors, physical transformation induced by the environment during storage and application compounds the complexity of the nanocrystal surface, particularly for kinetic products prone to shape deformation and surface reconstruction. Since metal nanocrystals are typically synthesized in an oxygenated environment using halide-based precursors, oxidative etching is inevitable if they are stored inside the reaction solution for an extended duration. When activated in suitable conditions, this mechanism can modify or remove surface features (e.g., corner/edge truncation, change in internal structure) since defect zones, corners, and edges possess higher surface energies, which are more susceptible to O_2 oxidization and dissolution [21]. A recent study examined the etching kinetics by monitoring the shape evolution of a Au nanocube in a controlled redox environment, providing insights into the reactivities of different surface atoms (Figure 5C–E) [95]. During etching, a tetrahexahedron was consistently observed as an intermediate, owing to a step-recession mechanism where peripheral edge atoms (CN <6) were preferentially etched compared with interior atoms. Regarding catalytic applications, elevated temperature and/or specific gases used during the operation can cause dramatic changes to the surface, impacting the nanocrystal's performance [96]. Altogether, the dynamic nature of surface heterogeneity during nanocrystal growth, storage, and application presents both challenges and opportunities for the design of catalytic materials.

Concluding remarks

Thanks to advances in synthetic and characterization techniques, the surface heterogeneity of nanocrystals has transformed into a powerful handle that can be harnessed to direct the shape evolution of nanocrystals, thus tailoring their properties for various applications. By leveraging surface heterogeneity and controlling experimental parameters, a nanocrystal's shape can be maneuvered via site-selected growth. The intricate balance between atomic deposition at preferential sites and surface diffusion is crucial in determining surface heterogeneity and guiding the growth pattern toward different products. Despite significant progress, several scientific problems or technical challenges persist, such as: the lack of quantitative analysis of deposition and

Outstanding questions

What are the key experimental conditions, growth parameters, and strategies required to achieve precise control over surface heterogeneity across various metal nanocrystal systems? How can large-scale production of nanocrystals with well-defined shapes and structures be realized to bridge academic studies and industrial applications?

Is there any difference in selectivity between metal ions and atoms when they deposit onto different regions of a seed? Which factors contribute to this selectivity, including the influence of capping agents, their adsorption and desorption phenomena, and surface features such as high-density vertices, edges, facets, and twin boundaries?

What is the explicit status of capping agents on the surface of seeds during the growth process? Is there any adsorption and desorption between capping agents and seeds, and how do these phenomena impact the surface heterogeneity of metal nanocrystals?

How can we design *in situ* experiments that enable direct observation of atomic behaviors such as surface diffusion and deposition processes during nanocrystal growth?

How can we establish a more quantitative approach to analyze the activation energies for surface diffusion and atom deposition processes across the different regions of nanocrystals?

How do distinct surface features, such as high-density vertices, edges, facets, and twin boundaries, influence the adsorption and reactivity of various substrates in catalytic processes? How can surface heterogeneity be harnessed to design metal nanocrystals with enhanced photocatalytic, electrocatalytic, and other functional properties?

In what way does surface heterogeneity affect the long-term stability and durability of metal nanocrystals in various catalytic and functional applications and what strategies can be employed to mitigate any detrimental effects?

diffusion rates for better control of the growth pattern [97,98]; the constant demand for cutting-edge characterization tools to resolve the atomistic details during nanocrystal growth [99]; and the pursuit of deeper insights into the influence of surface heterogeneity on the catalytic applications of nanocrystals [100] (see Outstanding questions).

Ultimately, the quest for next-generation catalysts with high activity and selectivity will rely on our fundamental understanding and precise control of surface heterogeneity on metal nanocrystals. We hope this review can inspire further inquiries and innovations in understanding, controlling, and harnessing the dynamic surface structures of metal nanocrystals, facilitating the rational development of advanced catalytic materials.

Acknowledgments

This work was supported by the National Science Foundation (NSF) under grants CBET-2219546 and CHE-2105602. Q.N.N. acknowledges a Graduate Research Fellowship from the NSF (DGE-2039655).

Declaration of interests

The authors declare no competing financial interest.

References

1. Thomas, J.M. and Thomas, W.J. (2015) *Principles and practice of heterogeneous catalysis*, Wiley
2. Vogt, C. and Weckhuysen, B.M. (2022) The concept of active site in heterogeneous catalysis. *Nat. Rev. Chem.* 6, 89–111
3. Munnik, P. *et al.* (2015) Recent developments in the synthesis of supported catalysts. *Chem. Rev.* 115, 6687–6718
4. Jorgensen, M. and Gronbeck, H. (2018) The site-assembly determines catalytic activity of nanoparticles. *Angew. Chem. Int. Ed.* 57, 5086–5089
5. Gontard, L.C. *et al.* (2007) Aberration-corrected imaging of active sites on industrial catalyst nanoparticles. *Angew. Chem. Int. Ed.* 46, 3683–3685
6. Kim, S. *et al.* (2021) Correlating 3D surface atomic structure and catalytic activities of Pt nanocrystals. *Nano Lett.* 21, 1175–1183
7. Somorjai, G.A. and Li, Y. (2011) Impact of surface chemistry. *Proc. Natl. Acad. Sci. U. S. A.* 108, 917–924
8. Ertl, G. (2008) Reactions at surfaces: from atoms to complexity (Nobel Lecture). *Angew. Chem. Int. Ed.* 47, 3524–3535
9. Gómez-Marín, A.M. and Feliu, J.M. (2015) Oxygen reduction on nanostructured platinum surfaces in acidic media: promoting effect of surface steps and ideal response of Pt(111). *Catal. Today* 244, 172–176
10. Bagger, A. *et al.* (2019) Electrochemical CO_2 reduction: classifying Cu facets. *ACS Catal.* 9, 7894–7899
11. Su, M. *et al.* (2020) *In situ* Raman study of CO electrooxidation on Pt (hkl) single-crystal surfaces in acidic solution. *Angew. Chem. Int. Ed.* 59, 23554–23558
12. Xia, Y. *et al.* (2009) Shape-controlled synthesis of metal nanocrystals: simple chemistry meets complex physics? *Angew. Chem. Int. Ed.* 48, 60–103
13. Cargnello, M. (2019) Colloidal nanocrystals as building blocks for well-defined heterogeneous catalysts. *Chem. Mater.* 31, 576–596
14. Shi, Y. *et al.* (2021) Noble-metal nanocrystals with controlled shapes for catalytic and electrocatalytic applications. *Chem. Rev.* 121, 649–735
15. Huo, D. *et al.* (2019) One-dimensional metal nanostructures: from colloidal syntheses to applications. *Chem. Rev.* 119, 8972–9073
16. Chen, Y. *et al.* (2018) Two-dimensional metal nanomaterials: synthesis, properties, and applications. *Chem. Rev.* 118, 6409–6455
17. Chen, Q. *et al.* (2016) Well-faceted noble-metal nanocrystals with nonconvex polyhedral shapes. *Chem. Soc. Rev.* 45, 3207–3220
18. Scarabelli, L. *et al.* (2023) Plate-like colloidal metal nanoparticles. *Chem. Rev.* 123, 3493–3542
19. Jeong, S. *et al.* (2022) Unraveling the structural sensitivity of CO_2 electroreduction at facet-defined nanocrystals via correlative single-entity and macroelectrode measurements. *J. Am. Chem. Soc.* 144, 12673
20. Kim, B.H. *et al.* (2020) Critical differences in 3D atomic structure of individual ligand-protected nanocrystals in solution. *Science* 368, 60–67
21. Xia, Y. *et al.* (2017) Seed-mediated growth of colloidal metal nanocrystals. *Angew. Chem. Int. Ed.* 56, 60–95
22. Nguyen, Q. *et al.* (2023) Colloidal synthesis of metal nanocrystals: from asymmetrical growth to symmetry breaking. *Chem. Rev.* 123, 3693–3760
23. She, Z.W. *et al.* (2017) Combining theory and experiment in electrocatalysis: insights into materials design. *Science* 355, eaad4998
24. Xie, C. *et al.* (2020) Surface and interface control in nanoparticle catalysis. *Chem. Rev.* 120, 1184–1249
25. Yuan, Y. *et al.* (2012) Advances in the rational design of rhodium nanoparticle catalysts: control via manipulation of the nanoparticle core and stabilizer. *ACS Catal.* 2, 1057–1069
26. Li, D. *et al.* (2014) Functional links between Pt single crystal morphology and nanoparticles with different size and shape: the oxygen reduction reaction case. *Energy Environ. Sci.* 7, 4061–4069
27. Zhu, W. *et al.* (2013) Monodisperse Au nanoparticles for selective electrocatalytic reduction of CO_2 to CO. *J. Am. Chem. Soc.* 135, 16833–16836
28. Deng, X. *et al.* (2022) Resolving the size-dependent transition between CO_2 reduction reaction and H_2 evolution reaction selectivity in sub-5 nm silver nanoparticle electrocatalysts. *ACS Catal.* 12, 5921–5929
29. Perez-Alonso, F.J. *et al.* (2012) The effect of size on the oxygen electroreduction activity of mass-selected platinum nanoparticles. *Angew. Chem. Int. Ed.* 51, 4641–4643
30. Tritsaris, G.A. *et al.* (2011) Atomic-scale modeling of particle size effects for the oxygen reduction reaction on Pt. *Catal. Lett.* 141, 909–913
31. Dong, C. *et al.* (2018) Size-dependent activity and selectivity of carbon dioxide photocatalytic reduction over platinum nanoparticles. *Nat. Commun.* 9, 1252
32. Wu, T. *et al.* (2022) Size effects of electrocatalysts: more than a variation of surface area. *ACS Nano* 16, 8531–8539
33. Carvalho, O.Q. *et al.* (2020) Understanding the role of surface heterogeneities in electrosynthesis reactions. *iScience* 23, 101814
34. Li, W. *et al.* (2020) Defect engineering for fuel-cell electrocatalysts. *Adv. Mater.* 32, 1907879

35. Lim, B. *et al.* (2010) New insights into the growth mechanism and surface structure of palladium nanocrystals. *Nano Res.* 3, 180–188
36. Andoy, N.M. *et al.* (2013) Single-molecule catalysis mapping quantifies site-specific activity and uncovers radial activity gradient on single 2D nanocrystals. *J. Am. Chem. Soc.* 135, 1845–1852
37. Zhang, Y. *et al.* (2015) Superresolution fluorescence mapping of single-nanoparticle catalysts reveals spatiotemporal variations in surface reactivity. *Proc. Natl. Acad. Sci. U. S. A.* 112, 8959–8964
38. Ow, M.J.K. *et al.* (2020) Super-resolution fluorescence microscopy reveals nanoscale catalytic heterogeneity on single copper nanowires. *ACS Appl. Nano Mater.* 3, 3163–3167
39. Dubau, L. *et al.* (2016) Defects do catalysis: CO monolayer oxidation and oxygen reduction reaction on hollow PtNi/C nanoparticles. *ACS Catal.* 6, 4673–4684
40. Wang, Y. *et al.* (2015) Use of reduction rate as a quantitative knob for controlling the twin structure and shape of palladium nanocrystals. *Nano Lett.* 15, 1445–1450
41. Yu, N.-F. *et al.* (2019) Pd nanocrystals with continuously tunable high-index facets as a model nanocatalyst. *ACS Catal.* 9, 3144–3152
42. Lee, H.-E. *et al.* (2015) Concave rhombic dodecahedral Au nanocatalyst with multiple high-index facets for CO_2 reduction. *ACS Nano* 9, 8384–8393
43. Vara, M. and Xia, Y. (2018) Facile synthesis of Pd concave nanocubes: from kinetics to mechanistic understanding and rationally designed protocol. *Nano Res.* 11, 3122–3131
44. Qian, J. *et al.* (2018) Synthesis of Pt nanocrystals with different shapes using the same protocol to optimize their catalytic activity toward oxygen reduction. *Mater. Today* 21, 834–844
45. Calle-Vallejo, F. *et al.* (2015) Finding optimal surface sites on heterogeneous catalysts by counting nearest neighbors. *Science* 350, 185–189
46. Sánchez-Iglesias, A. *et al.* (2006) Synthesis and optical properties of gold nanodecahedra with size control. *Adv. Mater.* 18, 2529–2534
47. Janssen, A. *et al.* (2021) Colloidal metal nanocrystals with metastable crystal structures. *Angew. Chem. Int. Ed.* 60, 12192–12203
48. Huang, H. *et al.* (2017) Understanding of strain effects in the electrochemical reduction of CO_2: using Pd nanostructures as an ideal platform. *Angew. Chem. Int. Ed.* 56, 3594–3598
49. Yang, T.-H. *et al.* (2020) Surface capping agents and their roles in shape-controlled synthesis of colloidal metal nanocrystals. *Angew. Chem. Int. Ed.* 59, 15378–15401
50. Qi, X. *et al.* (2015) How structure-directing agents control nanocrystal shape: polyvinylpyrrolidone-mediated growth of Ag nanocubes. *Nano Lett.* 15, 7711–7717
51. Zhang, Q.A. *et al.* (2011) Systematic study of the synthesis of silver nanoplates: is citrate a "magic" reagent? *J. Am. Chem. Soc.* 133, 18931–18939
52. Ruditskiy, A. and Xia, Y. (2016) Toward the synthesis of sub-15 nm Ag nanocubes with sharp corners and edges: the roles of heterogeneous nucleation and surface capping. *J. Am. Chem. Soc.* 138, 3161–3167
53. Lu, L. *et al.* (2021) The critical impacts of ligands on heterogeneous nanocatalysis: a review. *ACS Catal.* 11, 6020–6058
54. Yang, T.-H. *et al.* (2017) Toward a quantitative understanding of the reduction pathways of a salt precursor in the synthesis of metal nanocrystals. *Nano Lett.* 17, 334–340
55. Thanh, N.T.K. *et al.* (2014) Mechanisms of nucleation and growth of nanoparticles in solution. *Chem. Rev.* 114, 7610–7630
56. Yin, X. *et al.* (2017) Quantitative analysis of different formation modes of platinum nanocrystals controlled by ligand chemistry. *Nano Lett.* 17, 6146–6150
57. Yang, T.H. *et al.* (2017) Autocatalytic surface reduction and its role in controlling seed-mediated growth of colloidal metal nanocrystals. *Proc. Natl. Acad. Sci. U. S. A.* 114, 13619–13624
58. Figueroa-Cosme, L. *et al.* (2018) Synthesis of palladium nanoscale octahedra through a one-pot, dual-reductant route and kinetic analysis. *Chem. Eur. J.* 24, 6133–6139
59. Yang, T.-H. *et al.* (2020) Quantitative analysis of the multiple roles played by halide ions in controlling the growth patterns of palladium nanocrystals. *ChemNanoMat* 6, 576–588
60. Kolasinki, K.W. (2008) *Surface science: foundations of catalysis and nanoscience* (2nd edn), Wiley
61. Peng, H.-C. *et al.* (2016) Seed-mediated synthesis of Pd nanocrystals: the effect of surface capping on the heterogeneous nucleation and growth. *J. Phys. Chem. C* 120, 11754–11761
62. Smith, J.D. *et al.* (2020) Defect-directed growth of symmetrically branched metal nanocrystals. *Angew. Chem. Int. Ed.* 59, 943–950
63. Zheng, G.C. *et al.* (2020) Pd–Au heteropentamers: selective growth of Au on Pd tetrahedral nanoparticles with enhanced electrocatalytic activity. *Cryst. Growth Des.* 20, 5863–5867
64. Lyu, Z. *et al.* (2021) Kinetically controlled synthesis of Pd–Cu Janus nanocrystals with enriched surface structures and enhanced catalytic activities toward CO_2 reduction. *J. Am. Chem. Soc.* 143, 149–162
65. Xia, Y. *et al.* (2015) Shape-controlled synthesis of colloidal metal nanocrystals: thermodynamic versus kinetic products. *J. Am. Chem. Soc.* 137, 7947–7966
66. Ma, X. *et al.* (2020) Unveiling growth pathways of multiply twinned gold nanoparticles by *in situ* liquid cell transmission electron microscopy. *ACS Nano* 14, 9594–9604
67. Iqbal, M. *et al.* (2021) In search of excellence: convex versus concave noble metal nanostructures for electrocatalytic applications. *Adv. Mater.* 33, e2004554
68. Yang, T.H. *et al.* (2021) Noble-metal nanoframes and their catalytic applications. *Chem. Rev.* 121, 796–833
69. Xia, X. *et al.* (2011) Silver nanocrystals with concave surfaces and their optical and surface-enhanced Raman scattering properties. *Angew. Chem. Int. Ed.* 50, 12542–12546
70. Su, N. *et al.* (2016) Formation of palladium concave nanocrystals via auto-catalytic tip overgrowth by interplay of reduction kinetics, concentration gradient and surface diffusion. *Nanoscale* 8, 8673–8680
71. Park, J. *et al.* (2016) Platinum cubic nanoframes with enhanced catalytic activity and durability toward oxygen reduction. *ChemSusChem* 9, 2855–2861
72. Xie, S. *et al.* (2013) Synthesis of rhodium concave tetrahedrons by collectively manipulating the reduction kinetics, facet-selective capping, and surface diffusion. *Nano Lett.* 13, 6262–6268
73. Zhang, J. *et al.* (2016) Ag@Au concave cuboctahedra: a unique probe for monitoring Au-catalyzed reduction and oxidation reactions by surface-enhanced Raman spectroscopy. *ACS Nano* 10, 2607–2616
74. Ahn, J. *et al.* (2017) Site-selective carving and co-deposition: transformation of Ag nanocubes into concave nanocrystals encased by Au–Ag alloy frames. *ACS Nano* 12, 298–307
75. Lv, T. *et al.* (2016) Controlling the growth of Au on icosahedral seeds of Pd by manipulating the reduction kinetics. *J. Phys. Chem. C* 120, 20768–20774
76. Zhang, Z. *et al.* (2020) pH regulated synthesis of monodisperse penta-twinned gold nanoparticles with high yield. *Chem. Mater.* 32, 5626–5633
77. Zhang, T. *et al.* (2021) A universal route with fine kinetic control to a family of penta-twinned gold nanocrystals. *Chem. Sci.* 12, 12631–12639
78. Liu, M. *et al.* (2021) Twin-directed deposition of Pt on Pd icosahedral nanocrystals for catalysts with enhanced activity and durability toward oxygen reduction. *Nano Lett.* 21, 2248–2254
79. Li, Y. *et al.* (2021) Corner-, edge-, and facet-controlled growth of nanocrystals. *Sci. Adv.* 7, eabf1410
80. Xia, X. *et al.* (2013) On the role of surface diffusion in determining the shape or morphology of noble-metal nanocrystals. *Proc. Natl. Acad. Sci. U. S. A.* 110, 6669–6673
81. Oura, K. *et al.* (2003) *Surface science: an introduction* (1st edn), Springer
82. Liu, M. *et al.* (2016) The effect of surface capping on the diffusion of adatoms in the synthesis of Pd@Au core–shell nanocrystals. *Chem. Commun.* 52, 13159–13162
83. Qiu, X. *et al.* (2023) Twin proliferation and prolongation under kinetic control: Pd–Au Janus icosahedra versus Pd@Au core–shell starfishes. *J. Am. Chem. Soc.* 145, 13400–13410
84. Zhu, C. *et al.* (2012) Kinetically controlled overgrowth of Ag or Au on Pd nanocrystal seeds: from hybrid dimers to nonconcentric and concentric bimetallic nanocrystals. *J. Am. Chem. Soc.* 134, 15822–15831

85. Peng, H.-C. *et al.* (2015) Toward a quantitative understanding of symmetry reduction involved in the seed-mediated growth of pd nanocrystals. *J. Am. Chem. Soc.* 137, 6643–6652
86. Mayer, M. *et al.* (2015) Controlled living nanowire growth: precise control over the morphology and optical properties of AgAuAg bimetallic nanowires. *Nano Lett.* 15, 5427–5437
87. Zhao, H. *et al.* (2022) Atomic-scale structure dynamics of nanocrystals revealed by *in situ* and environmental transmission electron microscopy. *Adv. Mater.* Published online September 25, 2022. https://doi.org/10.1002/adma.202206911
88. Choi, B.K. *et al.* (2023) Shape transformation mechanism of gold nanoplates. *ACS Nano* 17, 2007–2018
89. You, R. *et al.* (2022) Revealing surface restraint-induced hexagonal Pd nanocrystals via *in situ* transmission electron microscopy. *Nano Lett.* 22, 4333–4339
90. Gao, W. *et al.* (2021) Atomistic insights into the nucleation and growth of platinum on palladium nanocrystals. *Nat. Commun.* 12, 3215
91. Sun, M. *et al.* (2021) Understanding symmetry breaking at the single-particle level via the growth of tetrahedron-shaped nanocrystals from higher-symmetry precursors. *ACS Nano* 15, 15953–15961
92. Yang, T.-H. *et al.* (2021) Understanding the role of poly (vinylpyrrolidone) in stabilizing and capping colloidal silver nanocrystals. *ACS Nano* 15, 14242–14252
93. Chen, Z. *et al.* (2019) Revisiting the polyol synthesis of silver nanostructures: role of chloride in nanocube formation. *ACS Nano* 13, 1849–1860
94. Xia, X. *et al.* (2016) Quantifying the coverage density of poly(ethylene glycol) chains on the surface of gold nanostructures. *ACS Nano* 6, 512–522
95. Ye, X.C. *et al.* (2016) Single-particle mapping of nonequilibrium nanocrystal transformations. *Science* 354, 874–877
96. Avanesian, T. *et al.* (2017) Quantitative and atomic-scale view of CO-induced Pt nanoparticle surface reconstruction at saturation coverage via DFT calculations coupled with *in situ* TEM and IR. *J. Am. Chem. Soc.* 139, 4551–4558
97. Wang, Y. *et al.* (2020) Quantitative analysis of DNA-mediated formation of metal nanocrystals. *J. Am. Chem. Soc.* 142, 20368–20379
98. Tan, S.F. *et al.* (2018) *In situ* kinetic and thermodynamic growth control of Au–Pd core-shell nanoparticles. *J. Am. Chem. Soc.* 140, 11680–11685
99. Zhou, J. *et al.* (2019) Observing crystal nucleation in four dimensions using atomic electron tomography. *Nature* 570, 500–503
100. Xu, L. *et al.* (2023) Formation of active sites on transition metals through reaction-driven migration of surface atoms. *Science* 380, 70–76